J Mol Model (2011) 17:2631–2638
DOI 10.1007/s00894-011-0963-1

ORIGINAL PAPER

Computational analysis of aspartic protease plasmepsin II complexed with EH58 inhibitor: a QM/MM MD study

Natália de Farias Silva · Jerônimo Lameira · Cláudio Nahum Alves

Received: 14 September 2010 / Accepted: 5 January 2011 / Published online: 25 January 2011

Abstract Plasmepsin (PM) II is one of four enzymes in the food vacuole of *Plasmodium falciparum*. It has become an attractive target for combating malaria through research regarding its importance in the *P. falciparum* metabolism and life cycle, making it the target of choice for structure-based drug design. This paper reports the results of hybrid quantum mechanics / molecular mechanics (QM/MM) molecular dynamics (MD) simulations employed to study the details of the interactions established between PM II and N-(3–{(2-benzo[1, 3]dioxol-5-yl-ethyl)[3-(1-methyl-3-oxo-1,3-dihydro-isoindol-2-yl) propionyl]-amino}-1-benzyl-2-(hydroxyl-propyl)-4-benzyloxy-3,5dimethoxy-benzamide (EH58), a well-known potent inhibitor for this enzyme. Electrostatic binding free energy and energy terms decomposition have been computed for PM II complexed with the EH58 inhibitor. The results reveal that there is a strong interaction between Asp34, Val78, Ser79, Tyr192 and Asp214 residues and the EH58 inhibitor. In addition, we have computed the potential of the mean force (PMF) profile in order to assign the protonation state of the two catalytic aspartates in PM II-EH58 complex. The results indicate that the protonation of Asp214 favors a stable active site structure, which is consistent with our electrostatic binding free energy calculation and with previous published works.

Keywords EH58 · Malaria · Molecular Dynamics · Plasmepsin II · PMF · QM/MM

Introduction

At present, Malaria is the tropical disease that most severely afflicts the world population, affecting 300-660 million people worldwide, with around 2.5 million deaths per year, mainly among children [1, 2]. Data from WHO indicate that the most affected regions are Africa, parts of Asia, Central and South America and some Caribbean Islands, which together account for 40% of the world population [3].

Plasmodium malariae is a parasitic protozoan that causes malaria in humans. Four species are known: *P. malariae, P. vivax, P. ovale* and *P. falciparum,* the last being the most lethal cause of deaths [4]. The mosquito vector of the disease belongs to the genus *Anopheles*, which is transmitted to humans by female mosquitoes and the parasite causes the disease in its intra-erythrocytic stage, by degrading human hemoglobin capacity for reaching maturity and power [5].

Sequencing of *P. falciparum* genome has led to the identification of ten different genes that encode the Plasmepsins (PMs), numbered I to X [6]. PMs I-IV are located in the acid food vacuole and are active during the intra-erytrocytic stage of the life cycle by providing nutrients for growth of the parasite [7]. In particular, these enzymes are involved in degrading the host hemoglobin, making them potentially attractive targets for the design of new drugs [8]. Inhibitors of PMs with values of Ki namolars have been identified, with some being lethal to malaria parasite cultures [9–16].

PM II is the most studied among the PMs and is translated by an inactive zymogen (proenzyme). Activation is linked to

Electronic supplementary material The online version of this article (doi:10.1007/s00894-011-0963-1) contains supplementary material, which is available to authorized users.

N. de Farias Silva · J. Lameira · C. N. Alves (✉)
Laboratório de Planejamento e Desenvolvimento de Fármacos,
Instituto de Ciências Exatas e Naturais,
Universidade Federal do Pará, UFPA,
Rua Augusto Corrêa, 01, Guamá CEP,
66075-110, Belém, PA, Brazil
e-mail: nahum@ufpa.br

parts of the N-terminal cleavage. This maturation needs to change in this region of the enzyme in order to allow the formation of the catalytic site, Asp34 and Asp214 catalytic residues. One of the two catalytic aspartates is protonated, while the other is negatively charged [17, 18]. Using crystallographic techniques, Asojo and co-workers have reported PM II complexed with the N-(3-((2-benzo[1, 3]dioxol-5-yl-ethyl)[3-(1-methyl-3-oxo-1.3-dihydroisoindol-2-yl)-propionyl]-amino)-1-Benzyl-2-hydroxypropyl)-4-benzyloxy-3,5-dimethoxy-benzamide (EH58) as an inhibitor to the parasite *P. falciparum* [19].

Several computational methodologies, including molecular docking and molecular dynamics (classical MD) [17, 18, 20–27], simulations have been employed to elucidate the binding mode of PM inhibitors, and calculate the free energy profile for the catalytic mechanism [22]. Moreover, Friedman et al. used classical MD simulations to study the protonation state of the aspartates in PM II. The authors showed that the protonation of D214 favors a stable active site structure [17]. However to the best of our knowledge, our study is the first time that combined quantum mechanical/molecular mechanical (QM/MM) simulations have been reported for a PM II-inhibitor complex. In addition, ligand orientations as well as protein-ligand interaction modes are different from those used in classical MD simulations. In hybrid QM/MM methods the ligand or substrate species may be described by a QM model, while the protein and solvent environment is represented by means of MM force fields. This hybrid methodology avoids most of the work needed to obtain new force field parameters for each new functional group, such as the ones presented in these compounds. Treating the ligand quantum mechanically has the additional advantage of including quantum effects such as ligand polarization upon binding [28, 29]. This can be very important when highly polarizable groups are embedded in anisotropic environments, e.g., in metal-containing active sites. Moreover, because the largest part of the system is classically described, sufficient sampling can be obtained at a reasonable computational cost.

Recently, we have successfully employed the QM/MM method in studying protein-ligand interaction energies and HIV-1 IN inhibitor activity [28–33]. In this paper, we employed hybrid quantum mechanics / molecular mechanics (QM/MM) molecular dynamics (MD) simulations to study the details of the PM II-EH58 interaction and to determine electrostatic binding free energy of PM II complexed with EH58 inhibitor. Furthermore, we have computed the potential of mean force (PMF) profile to assign the protonation state of the two catalytic aspartates in PM II-EH58 complex. Finally, the contribution of individual residues to the total inhibitor-protein interaction energy has been computed between EH58 and some key residues inside the binding pocket.

Methods and materials

Computational methods

In the study reported here, the computational models for the QM/MM MD calculations were taken from the dimeric PM II-EH58 complex crystal structure with PDB code 1LF3 [19]. Because standard pKa values of ionizable groups can be shifted by local protein environments [34], an accurate assignment of the protonation states of all these residues at pH=7 was carried out by recalculating the standard pKa values of the titratable amino acids using the "cluster method" [34], as implemented by Field and co-workers [35]. According to this method, each titratable residue in the protein is perturbed by the electrostatic effect of the protein environment. We have also performed calculation of p*K*a values of aminoacids within the empirical *propKa* program of Jensen and co-workers [36]. Using the "cluster method" the Asp214 residue was found to be protonated, while using the *propKa* program Asp34 was found to be protonated (see the Supporting Information). Interestingly, Asp214 and Asp34 have been proposed as the catalytic residues, one of which is protonated while the other is negatively charged thus the correct protonation state to both these residues is essential for a realistic modeling of the bind site [17]. Therefore, in this report, we have modeled the PM II-EH58 complex using two state protonation: **A** model, protonating the Asp214 and **B** model protonating the Asp34 (see Figs. 1a and 2a). Results obtained with both methods for the remains residues provided the same protonation state, standard state, at the selected pH for the simulations.

After adding the hydrogen atoms to the full structure, optimization algorithms series (steepest descent conjugated gradient and L-BFGS-B [37]) were applied. To avoid a denaturization and artificial configurations of the protein structure, all the heavy atoms of the protein and the inhibitor were restrained by means of a Cartesian harmonic umbrella with a force constant of 1000 kJ mol^{-1} $Å^{-2}$. Afterward, the system was fully relaxed, but the peptidic backbone was restrained with a lower constant of 100 kJ mol^{-1} $Å^{-2}$. Next, the optimized protein was placed in a cubic box with pre-equilibrated waters (100 Å side), using the mass center of the complex as the geometrical center. Any water with an oxygen atom lying in a radius of 2.8 Å from a heavy atom of the protein was deleted. The remaining water molecules were then relaxed using the same optimization algorithms. Afterwards, 100 ps of hybrid QM/MM Langevin-Verlet molecular dynamics (MD) at 300 K and in a canonical thermodynamic ensemble (NVT) were used to equilibrate the model.

For the hybrid QM/MM MD calculations, we have two simulation models, as explained above for both the **A** and **B**

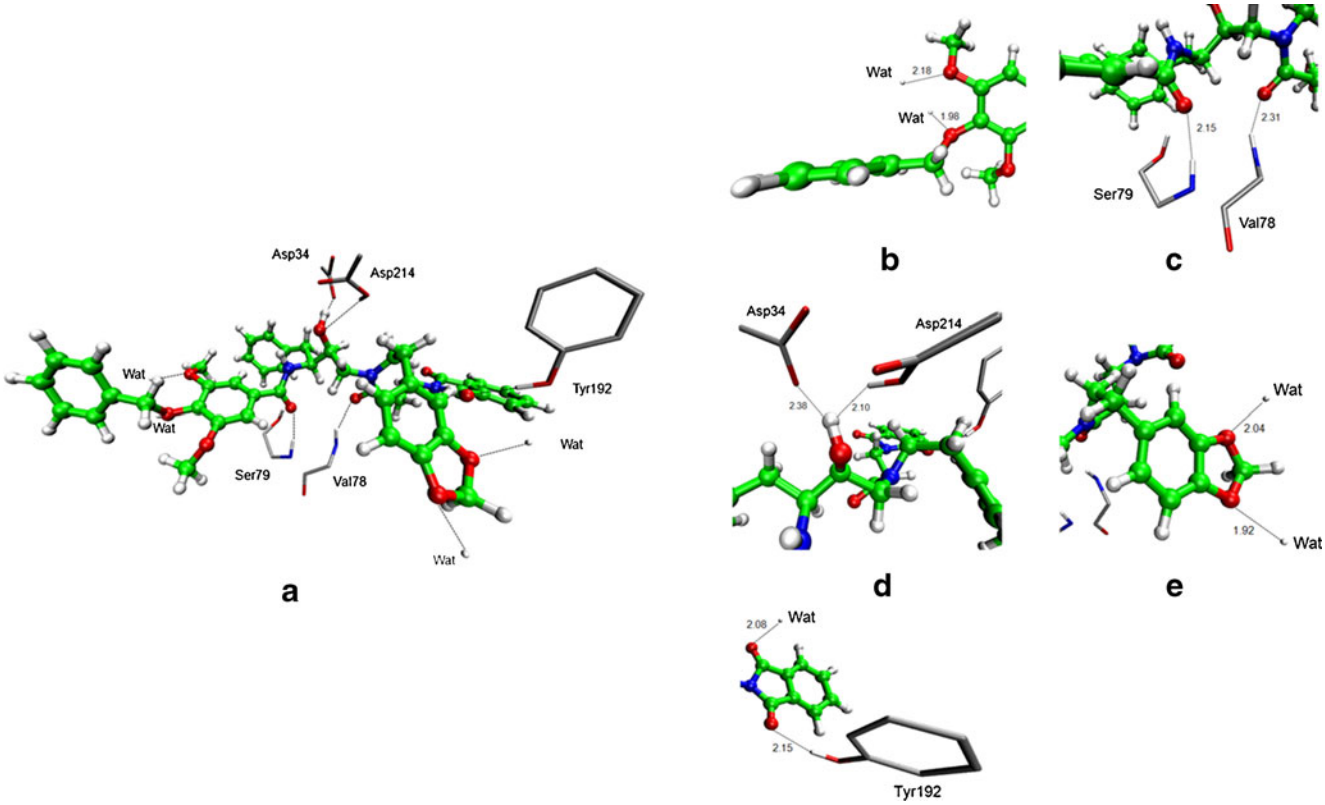

Fig. 1 (**a**) Structure of PM II-EH58 complex obtained after 1.6 ns of AM1/MM MD simulations and representation of the most important interactions (key interatomic distances, in Å) for **A** form. Details of interaction between: (**b**) EH58 and two waters; (**c**) EH58 and Ser79 and Val78; (**d**) EH58 and Asp34 and Asp214; (**e**) EH58 and two waters and (**f**) Tyr192 and water of crystallization

models (Figs. 1a and 2a); the atoms of the inhibitor and Asp214 and Asp34 were selected for treatment by QM. To saturate the valence of the QM/MM frontier in the first model, we used hydrogen atom as link atom [38, 39], placed between the C^{α} and C^{β} atoms of Asp214 and Asp34 residues. The resulting number of QM atoms was thus 113, while the final system contains 63.516 atoms in both models. Semiempirical AM1 Hamiltonian was employed to describe the QM part [40–42], while the rest of the system (protein plus water molecules) was described using the OPLS-AA [43] and TIP3P [44] force fields respectively, as implemented in the DYNAMO library [45, 46].

Due to the amount of degrees of freedom, any residue 25 Å apart from any of the atoms of the initial inhibitor was selected to be kept frozen (which represents 42.382 atoms) in the remaining calculations in order to make the model computationally feasible. Cutoffs for the non-bonding interactions were applied using a switching scheme, within a range radius from 18.0 to 14.5 Å.

Villar and co-workers have proposed that semi-empirical Austin Model 1 (AM1) is sufficient for use in the rational design of new drugs by comparing with B3LYP DFT method [47]. Recently, we have showed that interaction energy calculated with AM1/MM of PUGNAc in complex with *O*-GlcNAcase enzyme is correlated with B3LYP/MM [48]. In general, AM1/MM and DFT/MM calculations render quite similar results, thus confirming the reliability of the former [32, 48].

Once the systems were pre-equilibrated, 1.6 ns of AM1/MM MD were run at a temperature of 300 K. The computed RMSD for the protein during the last 100 ps always rendered a value below 0.9 Å, while the RMS of the temperature along the different equilibration steps was always lower than 2.5 K and the variation coefficient of the potential energy during the dynamics simulations was never higher than 0.3%. The potential energy of our scheme [49] is derived from the standard QM/MM formulation (for more details see Supplementary material). Finally, it must be pointed out that, since the use of high level Hamiltonians for performing hybrid MD is actually prohibitive, the electrostatic free energy has been evaluated using semiempirical AM1 Hamiltoninan. In addition, the interaction energy between the inhibitor and the environment was computed by residue (see Supplementary material), where the atoms of the inhibitor and Asp214 and Asp34 were selected to be treated by QM.

In order to obtain the free energy change associated to the proton transfer from Asp214 to Asp34 (i.e., the transformation between **A** and **B** forms), we have computed the corresponding potential of mean force (PMF) [50, 51] using the weighted histogram analysis method (WHAM)

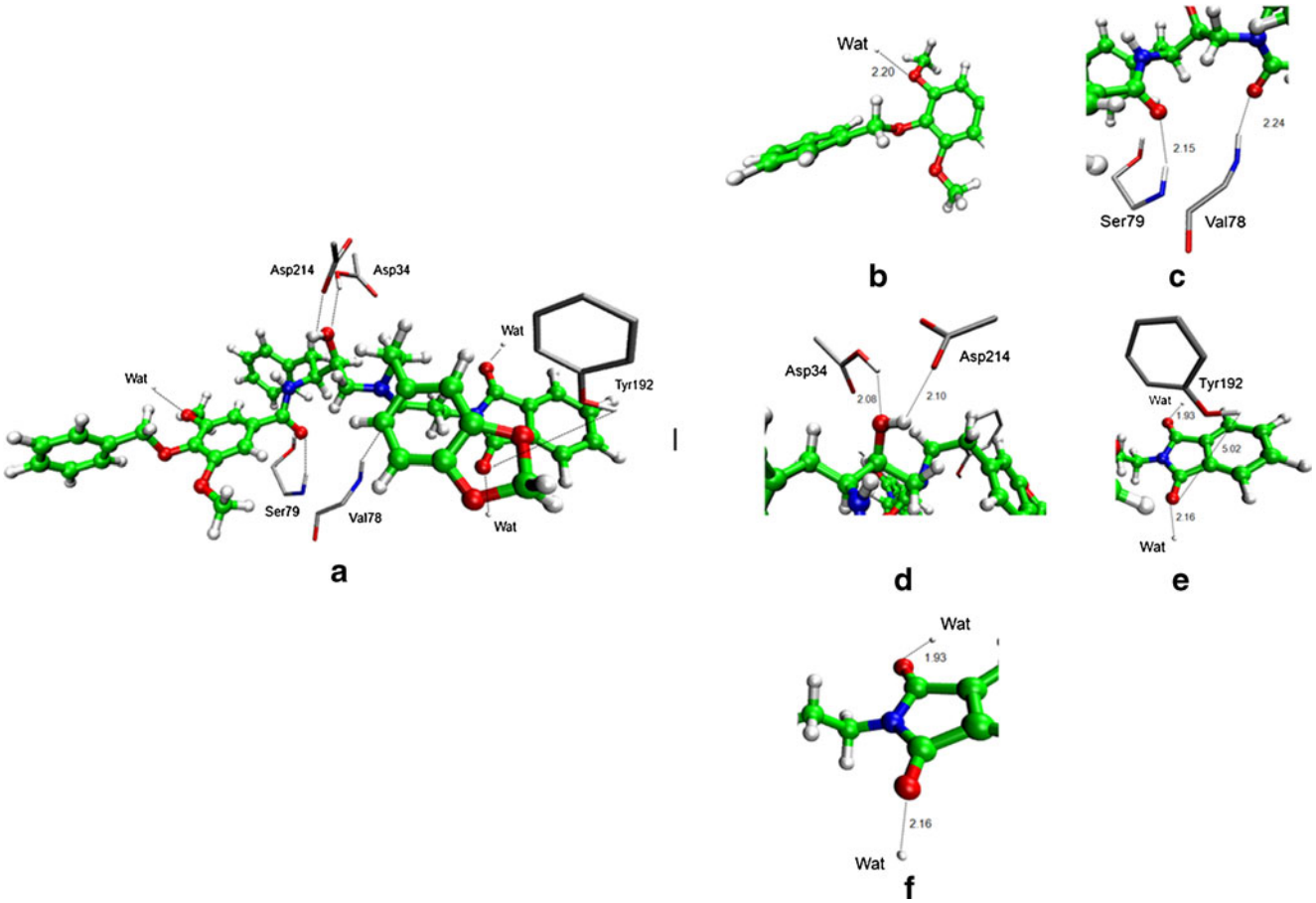

Fig. 2 Structures of PM II-EH58 complex obtained after 1.6 ns of AM1/MM MD simulations and representation of the most important interactions (key interatomic distances, in Å) for **B** form. Details of interaction between: (**b**) EH58 and two waters; (**c**) EH58 and Ser79 and Val78; (**d**) EH58 and Asp34 and Asp214; (**e**) EH58 and two waters and (**f**) Tyr192 and water of crystallization

combined with the umbrella sampling approach [52–54] as implemented in DYNAMO [45, 46]. In this PMF, the reaction coordinates distinguished was the antisymmetric combination of the distances HE2-OD2 of Asp214 (R1) and HE2-OD2 of Asp34 (R2) coordinates (Fig. 3) corresponding to the proton transfer from Asp214 to Asp34. A total of 60 simulations was performed at different values of R1 and R2 (in a range from -1.5 to +1.5 Å), with an umbrella force constant of 2800 kJ $\cdot mol^{-1} \cdot A^{-2}$. In each window, 5 ps of relaxation were followed by 10 ps of production with a time step of 0.5 ps due to the nature of the chemical step involving a hydrogen transfer. The Verlet algorithm was used to update the velocities at 300 K.

Results and discussion

As explained in the methodology section, we have modeled the PM II-EH58 complex using two models: **A** model with protonated Asp214 and **B** model with protonated Asp34 (see Figs. 1a and 2a). Hybrid AM1/MM MD simulations of 1.6 ns for PM II complexed with EH58 inhibitor have been performed. Averaged key substrate-protein distances for the PM II enzyme complex, computed over a series of 100,000 configurations from the last 100 ps of the QM/MM MD simulations, are shown in Figs. 1 and 2 for model **A** and **B**, respectively. Representative snapshots of the averaged structures of PM II obtained from the 1.6 ns MD simulations are shown in Fig. 1 for both models. As mentioned in the previous section, contribution of individual residues to the total inhibitor-protein interaction energy has been computed and the results are shown in Fig. 3 where negative values correspond to stabilizing effects; while binding free energies obtained from the electrostatic free energy perturbation (FEP) are reported in Table 1.

PM II-EH58 complex

Upon conclusion of the QM/MM MD simulations, several key interactions were found between the EH58 inhibitor and PM II. As can be seen from model **A** (Fig. 1d), the hydroxyl group interacts with the OD2 oxygen atom of

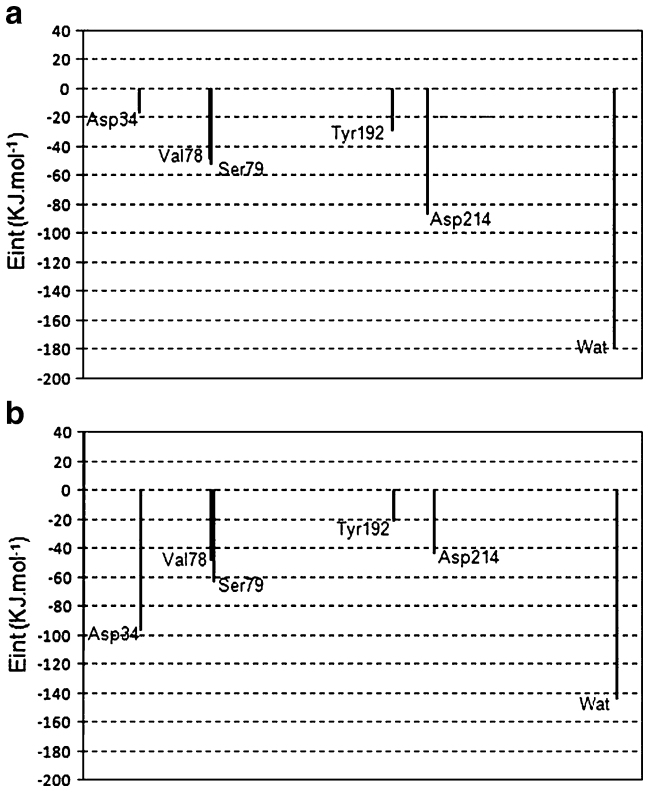

Fig. 3 Contributions of individual amino acid residues to inhibitor binding (in kJ ·mol^{-1}) from (**a**) **A** and (**b**) **B** structures obtained by means of QM/MM method. *water* refers to the effect of all the water molecules in the active site

Asp34 (2.10 Å) through a hydrogen bond. Furthermore, the hydroxyl group also presents a weaker hydrogen bond interaction with the protonated aspartic acid Asp214 (2.10 Å). Meanwhile, in model **B** (Fig. 2d), the hydroxyl group presents a weaker hydrogen bond interaction with the OD1 oxygen atom of Asp214 (2.10 Å) and accepts a weaker hydrogen bond from the Asp34 (2.38 Å). These interactions favor the stabilization of the protein-inhibitor complex as reflected in Fig. 3a and b. Consequently, we can say that the **A** model (protonating aspartic acid Asp214) provides better H-bonding, with the inhibitor sharing an ethylenediol transition state mimicking group.

As observed in Figs. 1 and 2, other important residues present a favorable interaction with the ligand, such as Val78, Ser79 and Tyr192. In the **A** model the flap residues Val78 and Ser79 form hydrogen bonds with EH58 at 2.31 Å and 2.15 Å (Fig. 1c). While in the **B** model Val78 and Ser79 residues form hydrogen bonds with EH58 at 2.24 Å and 2.15 Å (Fig. 2c), respectively. Additionally, the hydroxyl groups of Tyr192 form hydrogen bonds with the inhibitor at 2.15 Å in the **A** model (Fig. 1f) and 5.02 Å in the **B** model (Fig. 2d). As can be observed in Fig. 1, the principal structural difference between **A** and **B** models in the EH58-enzyme complex is found in the Tyr192 residue. X-ray crystallographic data [19] overall is not distant from both structures **A** and **B**. The RMSD differences between the corresponding C^{α} atom are 1.04 and 1.44 Å, for **A** and **B** models, respectively.

Finally, as observed in Figs. 1 and 2, there are some water molecules that interact with the inhibitor stabilizing the complex (Fig. 3a and b). These five water molecules contributed in stabilizing the EH58 inhibitor interaction at the active site of the protein through hydrogen bond-type ligand-water [55] in values 2.18 Å in O48 atom, 1.98 Å in O49 atom, 1.92 Å in O41 atom, 2.04 Å in O39 atom and 2.08 in O32 atom for **A** model (Fig. 1b, e and f). In **B** model, three water molecules contributed in stabilizing the ligand interaction at the active site of the protein through hydrogen bond-type ligand-water [55] in values 2.20 Å in O49 atom, 1.93 Å in O32 atom and 2.16 Å in O31atom (Fig. 2b, e and f). Recent reports have proposed that water molecules are important in the stabilization of the interaction between ligand and PM II [17, 24, 56] which agrees with our theoretical simulations.

Table 1 Binding free energies ($\Delta G_{Elect-QM/MM}$) obtained from the electrostatic FEP calculations at the AM1/MM level (values in kJ·mol^{-1}) for **A** form and **B** form

Model	$\Delta G_{Elect-QM/MM}$
A	-159.29
B	-143.68

Protonation state of PM-II

We have reported the linear correlation of p*K*a obtained using *propKa* program and "cluster method" for all aspartate residues in the supporting information. The results obtained with both methods are qualitatively in agreement for almost all residues (supporting information).

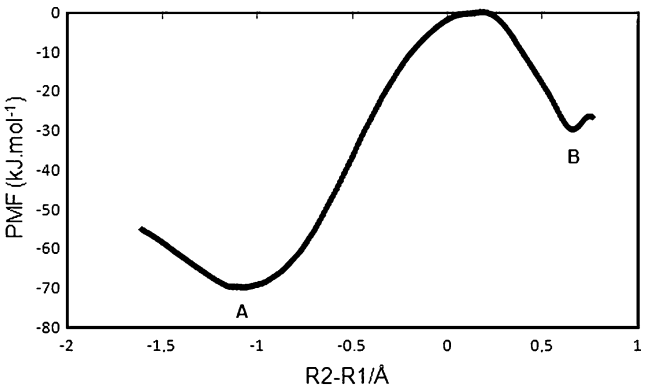

Fig. 4 Potential of mean force profile for proton transference from Asp214 to Asp34 (transformation between **A** and **B** forms). Relative energies in kJ·mol^{-1} and reaction coordinate (R1-R2) in Å

However, as commented in the methodology section, using the "cluster method" the Asp214 residue was found to be protonated, while using the *propKa* program Asp34 was found to be protonated. The protonation state of the catalytic aspartates in aspartic proteases is dependent on the presence and type of inhibitor bound, and it can thus be concluded that no unique model for describing the protonation state of some key aspartates such as the Asp214 and Asp34 is possible [17, 18, 24]. In this study, the electrostatic contribution to the protein-substrate interaction obtained from the free energy perturbation (FEP) calculations at AM1/MM level for **A** and **B** models reveals that the protonation of Asp214 leads to forming of a more stable PM II-HE58 complex than protonation of Asp34, which is consistent with previous publications [17, 18]. The difference observed between these models is 15.62 kJ mol^{-1} (see Table 1). Obviously, the FEP calculation is only one of the electrostatic contributions to the total binding free energy. Other terms such as the electrostatic contributions to the desolvation of the substrate and the protein may be important. Nevertheless, the former is constant for the experimental data analyzed here. The FEP might thus be used to examine which form (**A** or **B**) in the PM II-HE58 complex remains stable under the simulation conditions described above.

The protonation state of the catalytic aspartate has a strong influence on the presence or absence of the hydrogen bonds between some residues [17]. As can be observed in Fig. 3, the hydrogen bond between Asp34 and inhibitors is practically absent in model **B**. Thus, the loss of ligand-protein interaction, mainly through the electrostatic interactions between the Asp34 and the inhibitor in model **B**, could be responsible for the differences in the binding of free energy. Nevertheless, the comparison between both **A** and **B** models would require simulation of the protontransfer step between Asp214 and Asp34, as discussed below.

Based on the results and observations described above, we decided to trace the potential of mean force (PMF) corresponding to the proton transfer from the carboxylate oxygen atom OD2 of Asp214 to carboxylate oxygen atom OD2 of Asp34 (that is, from **A** to **B**). As shown in the PMF profile (Fig. 4), EH58-protein complex is more stable in the **A** form than in the **B** form by about 40 kJ·mol^{-1}, which is in accordance with the results binding free energies. The free energy barrier for the **A** to **B** conversion is of 70 kJ mol^{-1}. Thus, this result indicates that protonation of Asp214 favors a stable active site structure. This result is in agreement with previous HB analyses and the distributions of minimal distance between Oδs for PM II [17], which showed that the protonation of Asp214 is more consistent with the crystallographic data and catalytic mechanism.

Conclusions

In this study, hybrid QM/MM MD calculations have been carried out for PM II complexed with EH58 using two different forms for the PM II-EH58 complex; by protonating Asp214 or Asp34 (**A** and **B** models). The calculations allow one to determine the electrostatic contribution to the protein-ligand interaction free energies. The analysis of individual interactions between the inhibitor and the amino acids of the enzyme active site reveals how the influence of Asp34, Val78, Ser79, Tyr192 and Asp214 seems to be crucial, with the interactions established between the inhibitor and these residues being especially important. Moreover, it has been found that the protonation of Asp214 is a better model for this inhibitor in the active site of PM II. The prevalence of the **A** form has also been confirmed through tracing the free energy profile corresponding to the proton transfer between the carboxylate oxygen atom of Asp214 to the carboxylate oxygen atom of Asp34. It is expected that the results reported here will provide useful information for the rational design of new PM II inhibitors.

Acknowledgments The authors would like to thank Conselho Nacional Científico e Tecnológico, Coordenação de Aperfeiçoamento de Pessoal de Ensino Superior, Financiadora de Estudos e Projetos, Fundação de Amparo e Desenvolvimento da Pesquisa and Pró-Reitoria de Pesquisa e Pós-Graduação of Universidade Federal do Pará (Brazilian Agencies) for their financial support for this work.

References

1. Schlitzer M (2007) Malaria chemotherapeutics part 1: History of antimalarial drug development, currently used therapeutics, and drugs in clinical development. ChemMedChem 2:944–986
2. WHO (2007) fact sheet N8 94: available online: http://www.rollbackmalaria.org
3. Snow RW, Guerra CA, Noor AM, Myint HY, Hay SI (2005) Malaria risk - Reply. Nature 437:E4–E5
4. White NJ (1993) Malariology: Malaria parasites go ape. Lancet 341:793–793
5. França TCC, Santos MG, Figeiroa-Villar JD (2008) Malária: Aspectos Hitóricos e Quimioterapia. Quim Nova 31:1271–1278
6. Coombs GH, Goldberg DE, Klemba M, Berry C, Kay J, Mottram JC (2001) Aspartic proteases of *Plasmodium falciparum* and other parasitic protozoa as drug targets. Trends Parasitol 17:532–537
7. Francis SE, Sullivan DJ, Goldberg DE (1997) Hemoglobin metabolism in the malaria parasite *Plasmodium falciparum*. Annu Rev Microbiol 51:97–123
8. Banerjee R, Liu J, Beatty W, Pelosof L, Klemba M, Goldberg DE (2002) Four plasmepsins are active in the *Plasmodium falciparum* food vacuole, including a protease with an active-site histidine. Proc Natl Acad Sci USA 99:990–995
9. Carroll CD, Johnson TO, Tao S, Lauri G, Orlowski M, Gluzman IY, Goldberg DE, Dolle RE (1998) Evaluation of a structure-based statine cyclic diamino amide encoded combinatorial library against plasmepsin II and cathepsin D. Bioorg Med Chem Lett 8:3203–3206

10. Carroll CD, Orlowski M (1998) Screening aspartyl proteases with combinatorial libraries. Aspartic Prot 436:375–380
11. Carroll CD, Patel H, Johnson TO, Guo T, Orlowski M, He ZM, Cavallaro CL, Guo J, Oksman A, Gluzman IY, Connelly J, Chelsky D, Goldberg DE, Dolle RE (1998) Identification of potent inhibitors of *Plasmodium falciparum* plasmepsin II from an encoded statine combinatorial library. Bioorg Med Chem Lett 8:2315–2320
12. Goldberg DE, Slater AFG, Beavis R, Chait B, Cerami A, Henderson GB (1991) Hemoglobin degradation in the human malaria pathogen *Plasmodium-falciparum* - a catabolic pathway initiated by a specific aspartic protease. J Exp Med 173:961–969
13. Haque TS, Skillman AG, Lee CE, Habashita H, Gluzman IY, Ewing TJA, Goldberg DE, Kuntz ID, Ellman JA (1999) Potent, low-molecular-weight non-peptide inhibitors of malarial aspartyl protease plasmepsin II. J Med Chem 42:1428–1440
14. Silva AM, Lee AY, Erickson JW, Goldberg DE (1998) Structural analysis of plasmepsin II - A comparison with human aspartic proteases. Aspartic Prot 436:363–373
15. Silva AM, Lee AY, Gulnik SV, Majer P, Collins J, Bhat TN, Collins PJ, Cachau RE, Luker KE, Gluzman IY, Francis SE, Oksman A, Goldberg DE, Erickson JW (1996) Structure and inhibition of plasmepsin II, a hemoglobin-degrading enzyme from *Plasmodium falciparum*. Proc Natl Acad Sci USA 93:10034–10039
16. Westling J, Cipullo P, Hung SH, Saft H, Dame JB, Dunn BM (1999) Active site specificity of plasmepsin II. Protein Sci 8:2001–2009
17. Friedman R, Caflisch A (2007) The protonation state of the catalytic aspartates in plasmepsin II. FEBS Lett 581:4120–4124
18. Gutierrez-de-Teran H, Nervall M, Dunn BM, Clemente JC, Aqvist J (2006) Computational analysis of plasmepsin IV bound to an allophenylnorstatine inhibitor. FEBS Lett 580:5910–5916
19. Asojo OA, Gulnik SV, Afonina E, Yu B, Ellman JA, Haque TS, Silva AM (2003) Novel uncomplexed and complexed structures of plasmepsin II, an aspartic protease from *Plasmodium falciparum*. J Mol Biol 327:173–181
20. Andrews KT, Fairlie DP, Madala PK, Ray J, Wyatt DM, Hilton PM, Melville LA, Beattie L, Gardiner DL, Reid RC, Stoermer MJ, Skinner-Adams T, Berry C, McCarthy JS (2006) Potencies of human immunodeficiency virus protease inhibitors in vitro against *Plasmodium falciparum* and in vivo against murine malaria. Antimicrob Agents Chemother 50:639–648
21. Bjelic S, Aqvist J (2004) Computational prediction of structure, substrate binding mode, mechanism, and rate for a malaria protease with a novel type of active site. Biochemistry 43:14521–14528
22. Bjelic S, Aqvist J (2006) Catalysis and linear free energy relationships in aspartic proteases. Biochemistry 45:7709–7723
23. Bjelic S, Nervall M, Gutierrez-de-Teran H, Ersmark K, Hallberg A, Aqvist J (2007) Computational inhibitor design against malaria plasmepsins. Cell Mol Life Sci 64:2285–2305
24. Ersmark K, Feierberg I, Bjelic S, Hulten J, Samuelsson B, Aqvist J, Hallberg A (2003) C-2-symmetric inhibitors of Plasmodium falciparum plasmepsin II: Synthesis and theoretical predictions. Bioorg Med Chem 11:3723–3733
25. Kesavulu MM, Gowda ASP, Ramya TNC, Surolia N, Suguna K (2005) Plasmepsin inhibitors: design, synthesis, inhibitory studies and crystal structure analysis. J Pept Res 66:211–219
26. Muthas D, Noteberg D, Sabnis YA, Hamelink E, Vrang L, Samuelsson B, Karlen A, Hallberg A (2005) Synthesis, biological evaluation, and modeling studies of inhibitors aimed at the malarial proteases plasmepsins I and II. Bioorg Med Chem 13:5371–5390
27. Nezami A, Kimura T, Hidaka K, Kiso A, Liu J, Kiso Y, Goldberg DE, Freire E (2003) High-affinity inhibition of a family of *Plasmodium falciparum* proteases by a designed adaptive inhibitor. Biochemistry 42:8459–8464
28. Gao JL, Xia XF (1992) a priori evaluation of aqueous polarization effects through monte-carlo qm-mm simulations. Science 258:631–635
29. Senn HM, Thiel W (2009) QM/MM Methods for Biomolecular Systems. Angew Chem Int Ed 48:1198–1229
30. Alves CN, Marti S, Castillo R, Andres J, Moliner V, Tunon I, Silla E (2007) A quantum mechanics/molecular mechanics study of the protein-ligand interaction for inhibitors of HIV-1 integrase. Chem Eur J 13:7715–7724
31. Alves CN, Marti S, Castillo R, Andres J, Moliner V, Tunon I, Silla E (2007) Calculation of binding energy using BLYP/MM for the HIV-1 integrase complexed with the S-1360 and two analogues. Bioorg Med Chem 15:3818–3824
32. Alves CN, Marti S, Castillo R, Andres J, Moliner V, Tunon I, Silla E (2008) A quantum mechanic/molecular mechanic study of the wild-type and N155S mutant HIV-1 integrase complexed with diketo acid. Biophys J 94:2443–2451
33. Suresh CH, Vargheese AM, Vijayalakshmi KP, Mohan N, Koga N (2008) Role of structural water molecule in HIV protease-inhibitor complexes: A QM/MM study. J Comput Chem 29:1840–1849
34. Field M, David L, Rinado D (2006) Personal communication
35. Antosiewicz J, McCammon JA, Gilson MK (1994) Prediction of ph-dependent properties of proteins. J Mol Biol 238:415–436
36. Li H, Robertson AD, Jensen JH (2005) Very fast empirical prediction and rationalization of protein pK(a) values. Proteins 61:704–721
37. Byrd RH, Lu PH, Nocedal J, Zhu CY (1995) a limited memory algorithm for bound constrained optimization. SIAM J Sci Comput 16:1190–1208
38. Field MJ, Bash PA, Karplus M (1990) A combined quantum-mechanical and molecular mechanical potential for molecular-dynamics simulations. J Comput Chem 11:700–733
39. Singh UC, Kollman PA (1986) A combined abinitio quantum-mechanical and molecular mechanical method for carrying out simulations on complex molecular-systems - applications to the $CH_3Cl^+ Cl^-$ exchange-reaction and gas-phase protonation of polyethers. J Comput Chem 7:718–730
40. Dewar MJS, Zoebisch EG, Healy EF, Stewart JJP (1985) The development and use of quantum-mechanical molecular-models.76. AM1 - a new general-purpose quantum-mechanical molecular-model. J Am Chem Soc 107:3902–3909
41. Menikarachchi LC, Gascon JA (2010) QM/MM Approaches in Medicinal Chemistry Research. Curr Top Med Chem 10:46–54
42. Zhou T, Huang DZ, Caflisch A (2010) Quantum Mechanical Methods for Drug Design. Curr Top Med Chem 10:33–45
43. Jorgensen WL, Maxwell DS, TiradoRives J (1996) Development and testing of the OPLS all-atom force field on conformational energetics and properties of organic liquids. J Am Chem Soc 118:11225–11236
44. Jorgensen WL, Chandrasekhar J, Madura JD, Impey RW, Klein ML (1983) Comparison of simple potential functions for simulating liquid water. J Chem Phys 79:926–935
45. Field MJ (1999) Cambridge University Press: Cambridge UK
46. Field MJ, Albe M, Bret C, Proust-De Martin F, Thomas A (2000) The dynamo library for molecular simulations using hybrid quantum mechanical and molecular mechanical potentials. J Comput Chem 21:1088–1100
47. Villar R, Gil MJ, Garcia JI, Martinez-Merino V (2005) Are AM1 ligand-protein binding enthalpies good enough for use in the rational design of new drugs? J Comput Chem 26:1347–1358
48. Lameira J, Alves CN, Moliner V, Marti S, Kanaan N, Tunon I (2010) Quantum mechanics/molecular mechanics molecular dynamics simulation of wild-type and seven mutants of C*p*NagJ in complex with PUGNAc. J Phys Chem B 114:2090–2090

49. Lameira J, Alves CN, Moliner V, Marti S, Kanaan N, Tunon I (2008) A quantum mechanics/molecular mechanics study of the protein-ligand interaction of two potent inhibitors of human O-GlcNAcase: PUGNAc and NAG-Thiazoline. J Phys Chem B 112:14260–14266
50. McQuarrie DA (1976) Statistical Mechanics. Haper & Row, New York, p 266
51. Kirlwood JG (1935) Statistical Mechanics of Fluid Mixtures. J Chem Phys 3:300–312
52. Kumar S, Bouzida D, Swendsen RH, Kollman PA, Rosenberg JM (1992) The weighted histogram analysis method for free-energy calculations on biomolecules.1. The method. J Comput Chem 13:1011–1021
53. Roux B (1995) The calculation of the potential of mean force using computer simulations. Comput Phys Commun 91:275–282
54. Torrie GM, Valleau JP (1977) Non-physical sampling distributions in monte-carlo free-energy estimation - umbrella sampling. J Comput Phys 23:187–199
55. Yesudas JP, Sayyed FB, Suresh CH Analysis of structural water and CH···π interactions in HIV-1 protease and PTP1B complexes using a hydrogen bond prediction tool, HBPredicT. J Mol Model. doi:10.1007/s00894-010-0736-2
56. Luksch T, Chan NS, Brass S, Sotriffer CA, Klebe G, Diederich WE (2008) Computer-aided design and synthesis of nonpeptidic plasmepsin II and IV inhibitors. ChemMedChem 3:1323–1336